International Journal of Mechanical, Industrial and Aerospace Sciences
ISSN: 2517-9950
Vol:9, No:7, 2015

Numerical and Infrared Mapping of Temperature in Heat Affected Zone during Plasma Arc Cutting of Mild Steel

Dalvir Singh, Somnath Chattopadhyaya

***Abstract*—**During welding or flame cutting of metals, the prediction of heat affected zone (HAZ) is critical. There is need to develop a simple mathematical model to calculate the temperature variation in HAZ and derivative analysis can be used for this purpose. This study presents analytical solution for heat transfer through conduction in mild steel plate. The homogeneous and non-homogeneous boundary conditions are single variables. The full field analytical solutions of temperature measurement, subjected to local heating source, are derived first by method of separation of variables followed with the experimental visualization using infrared imaging. Based on the present work, it is suggested that appropriate heat input characteristics controls the temperature distribution in and around HAZ.

***Keywords*—**Conduction Heat Transfer, Heat Affected Zone (HAZ), Infra-Red Imaging, Numerical Method, Orthogonal Function, Plasma Arc Cutting, Separation of Variables, Temperature Measurement.

NOMENCLATURE

T	Temperature K
∂T	Temperature change K
k	Thermal conductivity W/m/K
q	Conductive heat transfer coefficient W/m^2/K
t	Plate thickness m
b	Plate breadth m
l	Length m
u'''	Internal energy per unit volume W/m^2/K
λ, μ, ψ	Eigen values
a, A, B, C	constants

I. INTRODUCTION

MEASUREMENT of temperature in today's industrial environment encompasses a wide variety of needs and applications. Temperature is a very critical and widely measured variable for most engineers. Many methods have been developed for measuring temperature. Most of these rely on measuring some physical property of a working material that varies with temperature. However, the analytical solution for the three dimensional heat conduction problems is available in the literature but to analyze some phenomena, we need to formulate some model for particular situations. There are many techniques to construct such models and finding their solution. For prediction of metal cutting and welding temperature conditions, there are many conduction heat transfer models available in the literature.

Arpasi [1] presented formulation and solutions of steady and unsteady one, two, and three-dimensional problems by applying various approaches. Barcza [2] presented a numerical method for solution of linear heat conduction equation known as weighing function method. He found that weighing function method is easy and efficient. Morini [3] presented an analytical approach to study the heat transfer for the dynamic and thermal fully developed region of rectangular ducts for different boundary conditions. He determined the two dimensional temperature distributions for adiabatic walls and finds the Nusselt numbers. Chang and Ma [4] developed an alternative analytical method to investigate the thermal conduction problem of a finite plate with multiple insulated cracks and they solve the differential equations by using Gauss integration. Dhawan and Kumar [5] derived differential equations for heat conduction in 2-D system and compared with finite element method using triangular and rectangular mesh. They found that the results obtained by FEM and exact solution were very close. Osman and Boucheffa [6] proposed an analytical model to compute the three-dimensional temperature distribution in a solid, subjected to a moving rectangular heat source with surface cooling. The model can be implemented in a thermo mechanical computational code to calculate the stress and deformation fields in a solid. Sonavane and Specht [7] developed a mathematical model for the temperature fluctuation in the wall of rotary kiln and predicted that temperature fluctuation decreases with increase in rotation speed of kiln, also found that temperature fluctuations does not depend on the diameter of rotary kiln. Further, heat conduction problems for various geometrical configurations with thermal or isothermal boundary conditions and solved by Lin [8]. He used Fourier transform technique in conjunction with the image method. Matian et al. [9] proposed computational model to study the heat generation and distribution in single-cell and two-cell polymer electrolyte membrane fuel cells stacks. Danish et al. [10] presented exact analytical solutions for different modes of heat transfer in the form of elementary algebraic and transcendental functions. The solutions provide better insight of the physical process and are valid for all parameter ranges unlike their approximate alternatives. Moreover, they are useful in judging the accuracy of other approximate solutions. Shahmardan et al. [11] developed an exact analytical solution for convective heat transfer in rectangular ducts. They obtained two identical

Singh Dalvir is with the Galgotia College of Engineering and Technology, Greater Noida, India (phone: 09910440723; e-mail:dalvir21@gmail.com).
Chattopadhyaya Somnath is with Indian School of Mines, Dhanbad, India (phone: 09431954821; e-mail: somuismu@gmail.com).

solutions for different sets of boundary conditions. The first solution is suitable for square cross section and another for rectangular cross section. Brubach et al. [12]) reviewed the basic principles of combustion and energy science. They proposed on surface temperature measurements with thermo graphic phosphors. Cotterell et al. [13] presented simplified models for strain and temperature measurement during orthogonal cutting process applying Ernst-Merchant theory and considering a 2-D steady state heat conduction problem. The results were validated with high speed imaging and Infrared imaging. Nikolay et al. [14] studied heat exchange near the liquid-gas interface by means of Background Oriented Schlieren and Infrared Thermal Imaging. They observed two different flow regimes in near-surface layer depending on the liquid properties and its initial temperature with respect to the ambient air. Salimi et al. [15] devised a novel analytical solution to the three-dimensional transient temperature field which can serve as a viable tool to predict the temperature distribution induced by a heat source, as a welding beam or tool, moving along the interface of a butt joint. They expressed the solution in the form of Green's function and compare the results with FEM. Yang et al. [16] presented a new approach using analytical expressions in the radial integration boundary element method (RIBEM) for solving three kinds of representative variable coefficient heat conduction problems. This approach can improve the computational efficiency considerably and can overcome the time-consuming deficiency of RIBEM in computing involved radial integrals.

The present study aims to develop a simple analytical solution for conduction heat transfer in mild steel plate of finite dimensions. The main objective is to predict the quantative analysis of temperature at any point on or inside the metal plates. Analytical model is developed using separation of variables followed by experimental verification with thermal imaging captured by infra-red imaging camera.

II. Formulation of the Conduction Problem [1]

A general problem may be formulated in either of the following forms:

(1) lumped or averaged
(2) distributed: (a) integral, (b) differential, (c) variational, (d) difference

Consider the three dimensional system as shown in Fig. 1. Assuming u''' is the internal energy per unit volume, q is the conduction heat transfer and k is the thermal conductivity of the system.

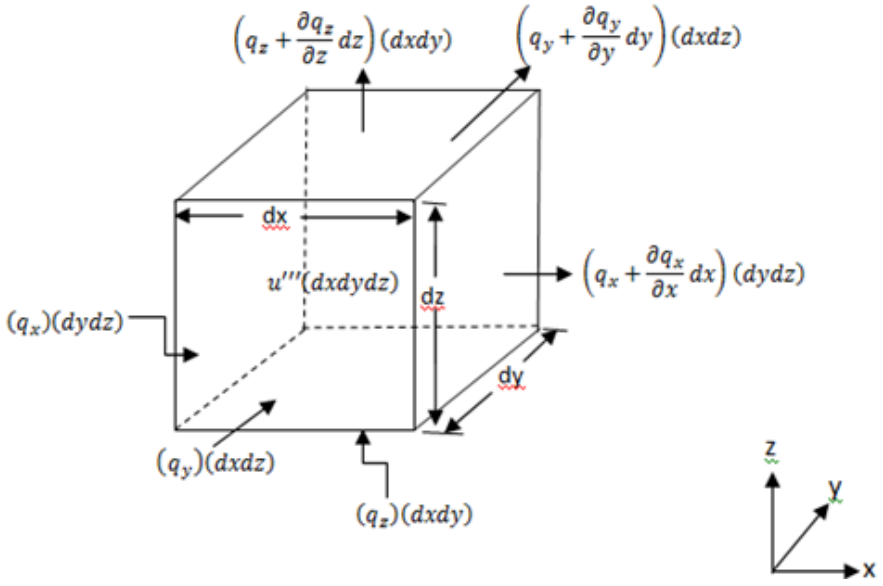

Fig. 1 A Three Dimensional System for Conduction Heat Transfer

Equation (1) is derived using the differential formulation and applying the first law of thermodynamics to the stated system.

$$q_x(dydz)-\left(q_x+\frac{\partial q_x}{\partial x}dx\right)(dydz)+q_y(dxdz)-\left(q_y+\frac{\partial q_y}{\partial y}dy\right)(dxdz)+q_z(dxdy)-\left(q_z+\frac{\partial q_z}{\partial z}dz\right)(dxdy)+u'''(dxdydz)=0$$

$$\text{or } \left(-\frac{\partial q_x}{\partial x}-\frac{\partial q_y}{\partial y}-\frac{\partial q_z}{\partial z}+u'''\right)dxdydz=0$$

$$\text{or } -\frac{\partial q_x}{\partial x}-\frac{\partial q_y}{\partial y}-\frac{\partial q_z}{\partial z}+u'''=0 \quad (1)$$

The three Cartesian components of the vectorial form of the Fourier's law to be used for isotropic continua are.

$$q_{x=-k\frac{\partial T}{\partial x}},\ q_{y=-k\frac{\partial T}{\partial y}},\ q_{z=-k\frac{\partial T}{\partial z}} \quad (2)$$

Using expression from (2) in (1) results (3), which further reduces to (4) while 'k' is constant

$$\frac{\partial}{\partial x}\left(k\frac{\partial T}{\partial x}\right)+\frac{\partial}{\partial y}\left(k\frac{\partial T}{\partial y}\right)+\frac{\partial}{\partial z}\left(k\frac{\partial T}{\partial z}\right)+u'''=0 \quad (3)$$

$$\frac{\partial^2 T}{\partial x^2}+\frac{\partial^2 T}{\partial y^2}+\frac{\partial^2 T}{\partial z^2}+\frac{u'''}{k}=0 \quad (4)$$

If internal energy is constant then u''' = 0. Then

$$\frac{\partial^2 T}{\partial x^2}+\frac{\partial^2 T}{\partial y^2}+\frac{\partial^2 T}{\partial z^2}=0 \quad (5)$$

III. Problem and Solution

Cuboidal piece of metal of length 'l', breadth '2b' and thickness '2t' is taken for analysis. Assuming that T_s is the surface temperature of material and T_a is the ambient temperature (Fig. 2). The differential formulation of the problem, according to the selected reference frame, is given by (5) subjected to following conditions:

$$\begin{aligned} &\frac{\partial T(0,y,z)}{\partial x}=0 \quad ; \quad T(b,y,z)=T_s \\ &\frac{\partial T(x,0,z)}{\partial y}=0 \quad ; \quad T(x,y,l)=T_s \\ &T(x,y,0)=T_s \quad ; \quad T(x,t,z)=T_a \end{aligned} \quad (6)$$

For using method of separation of variables, the differential equation and five boundary conditions must be homogeneous. Assuming $\theta = T - T_s$, then (5) transforms to (7)

$$\frac{\partial^2 \theta}{\partial x^2}+\frac{\partial^2 \theta}{\partial y^2}+\frac{\partial^2 \theta}{\partial z^2}=0 \quad (7)$$

Subjected to

$$\begin{aligned} &\frac{\partial \theta(0,y,z)}{\partial x}=0 \quad ; \quad \theta(b,y,z)=0 \\ &\frac{\partial \theta(x,0,z)}{\partial y}=0 \quad ; \quad \theta(x,y,l)=0 \\ &\theta(x,y,0)=T(x,y,0)-T_s=T_s-T_s=0 \\ &\theta(x,t,z)=T(x,t,z)-T_s=T_a-T_s=\theta_t \text{ (say)} \end{aligned}$$

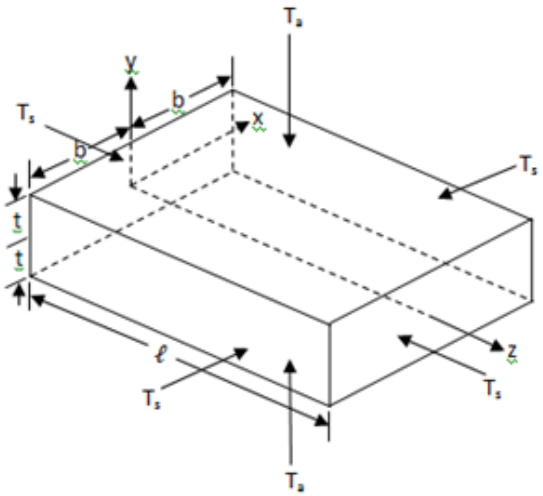

Fig. 2 A Cuboidal Test Element

Assuming a product solution of the form

$$\theta(x,y,z)=X(x)Y(y)Z(z) \quad (8)$$

Substituting (8) into (7) results

$$YZ\frac{d^2X}{dx^2}+XZ\frac{d^2Y}{dy^2}+XY\frac{d^2Z}{dz^2}=0$$

Dividing the above equation by 'XYZ' results

$$\begin{aligned} &\frac{1}{X}\frac{d^2X}{dx^2}+\frac{1}{Y}\frac{d^2Y}{dy^2}+\frac{1}{Z}\frac{d^2Z}{dz^2}=0 \\ &\text{or } -\frac{1}{X}\frac{d^2X}{dx^2}=\frac{1}{Y}\frac{d^2Y}{dy^2}+\frac{1}{Z}\frac{d^2Z}{dz^2}=\lambda^2 \end{aligned} \quad (9)$$

The first characteristic value problem in the x-direction is

$$\frac{d^2X}{dx^2}+\lambda^2 X=0 \quad (10)$$

The boundary conditions are calculated from (8) as follows

$$\begin{aligned} &\frac{\partial \theta(x,y,z)}{\partial x}=\frac{dX(x)}{dx}Y(y)Z(z) \\ &\frac{\partial \theta(0,y,z)}{\partial x}=\frac{dX(0)}{dx}Y(y)Z(z)=0 \text{ gives} \frac{dX(0)}{dx}=0 \\ &\theta(b,y,z)=X(b)Y(y)Z(z)=0 \text{ gives } X(b)=0 \end{aligned}$$

Further rearranging the second equality of (9) results

$$-\frac{1}{Z}\frac{d^2Z}{dz^2}=\frac{1}{Y}\frac{d^2Y}{dy^2}-\lambda^2=\mu^2 \quad (11)$$

Equation (11) gives the second characteristic value problem in y-direction as

$$\frac{d^2Y}{dy^2}-(\lambda^2+\mu^2)Y=0 \quad (12)$$

Subjected to

$$\frac{dY(0)}{dy}=0$$

The third characteristic value problem in z-direction is

$$\frac{d^2Z}{dz^2}+\mu^2 Z=0 \quad (13)$$

Subjected to $Z(0)=0$, $Z(\ell)=0$

The general solution of (10) is

$$\begin{aligned} X &= A_1 \sin\lambda x + A_2 \cos\lambda x \\ \frac{dX}{dx} &= A_1\lambda\cos\lambda x - A_2\lambda\sin\lambda x \end{aligned}$$

Application of first boundary condition: $\frac{dX(0)}{dx}=0$ leads to

$$\begin{aligned} &A_1\lambda\cos\lambda(0)-A_2\lambda\sin\lambda(0)=0 \\ &A_1\lambda=0 \\ &A_1=0 \end{aligned}$$

Therefore $X = A_2 \cos\lambda x$

Now applying second boundary condition: X(b) = 0

$$X(b) = A_2 \cos\lambda b = 0$$

$$\cos \lambda b = 0$$
$$\lambda b = \frac{\pi}{2}$$
or $\lambda_n b = (2n+1)\frac{\pi}{2}$; where n=0, 1, 2, 3……

Therefore solution of (10) is

$$X_n = A_n \phi_n(x) \quad (14)$$

where $\phi_n(x) = characteristicfunction = \cos \lambda_n x$. Now the general solution of (13) is

$$Z = B_1 \sin \mu z + B_2 \cos \mu z$$

Using first boundary condition: Z (0) = 0 leads $B_1 \sin \mu(0) + B_2 \cos \mu(0) = 0$. Gives $B_2 = 0$. Therefore $Z = B_1 \sin \mu z$. Now using second boundary condition: Z (ℓ) = 0

$$B_1 \sin \mu \ell = 0$$

Therefore $\sin \mu \ell = 0$ or $\mu_m \ell = m\pi$; where m = 0, 1, 2, 3……. Therefore the solution of (13) is

$$Z_m = B_m \psi_{m(z)} \quad (15)$$

where $\psi_m(z) = \sin \mu_m z$. Finally the solution of (12) is

$$Y_{mn} = C_{mn} e^{-(\lambda_n^2 + \mu_m^2)^{1/2} y} \quad (16)$$

Thus the product solution leads to

$$\theta(x,y,z) = \sum_{n=0}^{\infty} \sum_{m=0}^{\infty} a_{mn}\, e^{-(\lambda_n^2 + \mu_m^2)^{1/2} y} \cos \lambda_n x \sin \mu_m z \quad (17)$$

where $a_{mn} = A_n B_m C_{mn}$. Equation (12) by means of non-separable boundary condition: θ(x,t,z) = θ_i becomes

$$\theta_t = \sum_{n=0}^{\infty} \sum_{m=0}^{\infty} a_{mn}\, e^{-(\lambda_n^2 + \mu_m^2)^{1/2} t} \cos \lambda_n x \sin \mu_m z \quad (18)$$

Now multiply (18) by $\cos \lambda_p x \sin \mu_q z$ and integrating the result

$$\int_0^{\ell} \int_0^{b} \theta_t \cos \lambda_p x \sin \mu_q z \, dx dz$$
$$= \sum_{n=0}^{\infty} \sum_{m=0}^{\infty} a_{mn}\, e^{-(\lambda_n^2 + \mu_m^2)^{1/2} t} \int_0^{\ell} \int_0^{b} \cos \lambda_n x \sin \mu_m z \cos \lambda_p x \sin \mu_q z \, dx dz \quad (19)$$

Now using condition of orthogonality in both the x- and y-directions, the terms on the right of (19) are zero except the terms corresponding to p = n and q = m; hence

$$a_{mn} = \frac{\theta_t \int_0^{\ell} \int_0^{b} \cos \lambda_n x \sin \mu_m z \, dx dz}{e^{-(\lambda_n^2 + \mu_m^2)^{1/2} t} \int_0^{\ell} \int_0^{b} \cos^2 \lambda_n x \sin^2 \mu_m z \, dx dz} \quad (20)$$

Solving (20) results

$$a_{mn} = \frac{4\theta_t \sin \lambda_n b\,(1 - \cos \mu_m \ell)}{(\lambda_n b)(\mu_m \ell) e^{-(\lambda_n^2 + \mu_m^2)^{1/2} t}}$$

Substitution of $\lambda_n b = (2n+1)\frac{\pi}{2}$ and $\mu_m \ell = m\pi$ results

$$a_{mn} = \frac{4\theta_t (-1)^n [1-(-1)^m]}{(\lambda_n b)(\mu_m \ell) e^{-(\lambda_n^2 + \mu_m^2)^{1/2} t}} \quad (21)$$

Now substituting (21) into (17)

$$\theta(x,y,z) = \sum_{n=0}^{\infty} \sum_{m=0}^{\infty} \frac{4\theta_t (-1)^n [1-(-1)^m]}{(\lambda_n b)(\mu_m \ell) e^{-(\lambda_n^2 + \mu_m^2)^{1/2} (t-y)}} \cos \lambda_n x \sin \mu_m z \quad (22)$$

$$T(x, y, z) = \theta(x, y, z) + T_s \quad (23)$$

IV. Experimental

A. Materials

For temperature measurement, machined mild steel (MS) plates of dimensions: 150 mm x 100 mm x 16 mm are used. MS plates are well cleaned to ensure no surface variations and a uniform surface finish.

B. Instrumentation

The plates are cut by Plasma Cutting process. All the cuttings are made using a FLAMINGO Portable Shape Cutting machine of Hypertherm Powermax 45 suppliedby ESAB INDIA Ltd (Fig. 3). Arc current of 45 amps and arc voltage of 127 V DC are used. The electrodes used are T45m – 220669. Cutting is carried out in the vertical position with cutting speed of 320 mm/min.

Fig. 3 Plasma Cutting Machine

C. Thermal Imaging

Thermal imaging is carried out using an infrared camera (RayCAm C.A.1886, procured from CHAUVIN ARNOUX) (Fig. 4) with operating temperature of 25°C, the emissivity of 0.21 and operating humidity of 45%.

The infrared camera is used to capture thermal image manually from a distance of about 1.0 m from the mild steel plate and suitably focused so that the entire work piece could be seen immediately after cutting (Fig. 5). This makes it possible to observe the temperature distribution in the MS plate. The images are recorded and subsequently analyzed.

Fig. 4 Infra-Red Camera

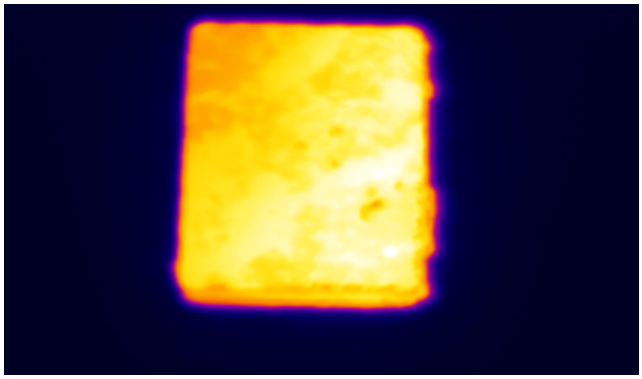

Fig. 5 Thermogram produced by thermal imaging camera

V. Results and Discussion

For predicting the temperature at various points, a MATLAB code is written and plotted as shown in Fig. 7. A Thermal image is captured using Thermal Imaging Camera in which maximum and minimum temperatures are shown (Fig. 5). Ray CAM Standard Software is used to calculate experimental values of temperature at different points (Fig. 6).

Fig. 6 shows the variation in temperature at different points and which is recorded experimentally. To explore the temperature variation throughout the cross-section, different points (numbered as P1, P1…P15) are selected and their temperature is mapped with the help of inbuilt software of Infrared camera (Fig. 7). The numerical solution of the derived equations is achieved by MATLAB code. The respective points are considered in MATLAB code and temperatures are calculated, as shown in Fig. 7. Also Fig.7 shows that there is marginal difference in theoretical and experimental values which is due to the time gap between cutting the plate and capturing the thermal image. This difference can be minimised by using online thermal imaging camera.

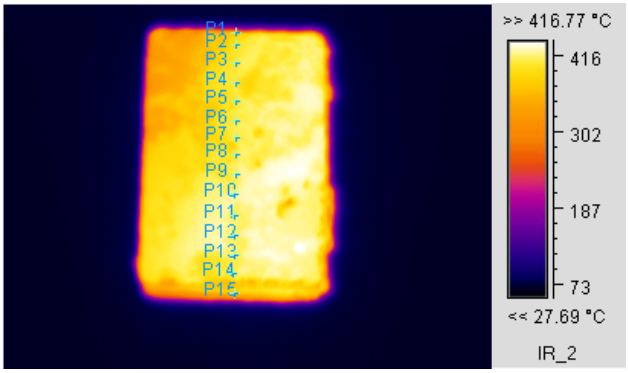

Fig. 6 Heat affected zone for 16 mm mild steel plate

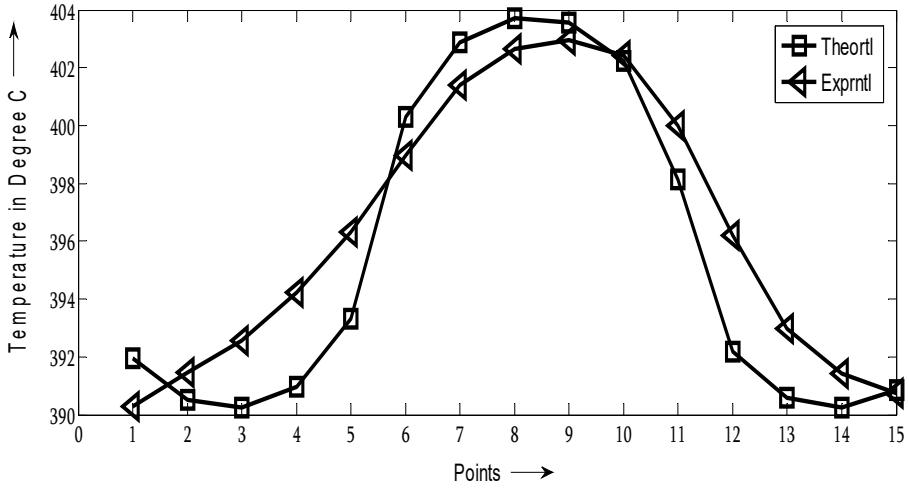

Fig. 7 Variation of Temperature at Different Points

VI. Conclusion and Future Direction of Research

The variation in temperature during cutting or welding can be mapped using infrared thermal imaging camera and the same can be predicted and verified by analytical technique. The model presented in this work is quite accurate in predicting the temperature and can be used instead of thermal imaging camera, which is a high cost set-up.

References

[1] Arpasi V.S. (1966) Conduction Heat Transfer. Copyright by Addison-Wesley. Printed in United States of America.

[2] Barcza J. (1993) A numerical method for solution of linear transient heat conduction equations. *Periodica Polytechnica Ser. Mech Engg Vol. 37:* 263–279.

[3] Morini G. L. (2000). Analytical determination of the temperature distribution and Nusselt numbers in rectangular ducts with constant axial heat flux. *International Journal of Heat and Mass Transfer43:* 741–755.

[4] Chang C. Y. & Ma C. C. (2001) Transient thermal conduction analysis of a rectangular plate with multiple insulated cracks by the alternating method. *International Journal of Heat and Mass Transfer44:* 2423–2437.

[5] Dhawan S. & Kumar S. (2009). A Comparative Study of Numerical Techniques for 2D Transient Heat Conduction Equation Using Finite Element Method. *International Journal of Research and Reviews in Applied Sciences ISSN: 2076-734X, EISSN: 2076-7366 Vol. 1 Issue 1: 38–46.*

[6] Osman, T. & Boucheffa A. (2009). Analytical solution for the 3D steady state conduction in a solid subjected to a moving rectangular heat source and surface cooling. *Comptes Rendus – Mecanique 337*(2): 107–111.

[7] Sonavane Y. & Specht E. (2009). Numerical Analysis of the Heat Transfer in the Wall of Rotary Kiln Using Finite Element Method Ansys. *Seventh International Conference on CFD in the Minerals and Process Industries*, (December), 1–5.

[8] Lin, R.-L. (2010). Explicit full field analytic solutions for two-dimensional heat conduction problems with finite dimensions. *International Journal of Heat and Mass Transfer*, *53*(9-10): 1882–1892.

[9] Matian M., Marquis A. J., & Brandon N. P. (2010). Application of thermal imaging to validate a heat transfer model for polymer electrolyte fuel cells. *International Journal of Hydrogen Energy*, *35*(22): 12308–12316

[10] Danish M., & Kumar S. (2011). Exact Analytical Solutions of Three Nonlinear Heat Transfer Models. *Proceedings of the World Congress on Engineering Vol.III.*

[11] Shahmardan M. M., Norouzi M., Kayhani M. H., & Amiri Delouei A. (2012). An exact analytical solution for convective heat transfer in rectangular ducts. *Journal of Zhejiang University SCIENCE ISSN: 1673-565X.*

[12] Brübach J., Pflitsch C., Dreizler A., & Atakan, B. (2013). On surface temperature measurements with thermographic phosphors: A review. *Progress in Energy and Combustion Science39:* 37–60.

[13] Cotterell, M., Ares, E., Yanes, J., López, F., Hernandez, P., & Peláez, G. (2013). Temperature and strain measurement during chip formation in orthogonal cutting conditions applied to Ti-6Al-4V. *Procedia Engineering63:* 922–930.

[14] Nikolay A. V., Alexander V. U., Yulia Y. P. (2014). Combined study of heat exchange near the liquid–gas interface by means of Background Oriented Schlieren and Infrared Thermal Imaging. *Experimental Thermal and Fluid Science 59:*238-245.

[15] Salimi S., Bahemmat P., & Haghpanahi M. (2014). A 3D transient analytical solution to the temperature field during dissimilar welding processes. *International Journal of Mechanical Sciences79:* 66–74.

[16] Yang K., Gao X., & Liu Y.F. (2014). New analytical expressions in radial integration BEM for solving heat conduction problems with variable coefficients. *Engineering Analysis with Boundary Elements 50:224-230.*